Bull Math Biol (2011) 73:2088–2108
DOI 10.1007/s11538-010-9612-6

ORIGINAL ARTICLE

Homogenization of Large-Scale Movement Models in Ecology

Martha J. Garlick · James A. Powell · Mevin B. Hooten · Leslie R. McFarlane

Received: 10 May 2010 / Accepted: 11 November 2010 / Published online: 1 January 2011

Abstract A difficulty in using diffusion models to predict large scale animal population dispersal is that individuals move differently based on local information (as opposed to gradients) in differing habitat types. This can be accommodated by using ecological diffusion. However, real environments are often spatially complex, limiting application of a direct approach. Homogenization for partial differential equations has long been applied to Fickian diffusion (in which average individual movement is organized along gradients of habitat and population density). We derive a homogenization procedure for ecological diffusion and apply it to a simple model for chronic wasting disease in mule deer. Homogenization allows us to determine the impact of small scale (10–100 m) habitat variability on large scale (10–100 km) movement. The procedure generates asymptotic equations for solutions on the large scale with parameters defined by small-scale variation. The simplicity of this homogenization procedure is striking when compared to the multi-dimensional homogenization procedure for Fickian diffusion,and the method will be equally straightforward for more complex models.

Keywords Chronic wasting disease · Diffusion model · Ecological diffusion · Homogenization · Multi-scale modeling · Spatial heterogeneity · Mule deer (*Odocoileus hemionus*)

M.J. Garlick (✉) · J.A. Powell
Department of Mathematics and Statistics, Utah State University, Logan, UT 84322, USA
e-mail: marti.garlick@aggiemail.usu.edu

M.B. Hooten
USGS Colorado Cooperative Fish and Wildlife Research Unit; Department of Fish, Wildlife, and Conservation Biology, Colorado State University, Fort Collins, CO 80523, USA

L.R. McFarlane
Utah Division of Wildlife Resources, Salt Lake City, UT 84114, USA

1 Introduction

Diffusion models have been applied to biological problems for many years. Fisher (1937) pioneered their use in genetics, while Turing (1952), Swindale (1980), and Murray (1980) are among many to use them to model pattern formation. Shellam (1951) greatly impacted mathematical modeling in ecology by combining the diffusive dispersal of organisms with population dynamics via reaction-diffusion equations of the form $\frac{\partial u}{\partial t} = D\nabla^2 u + f(u)$. Here D is the rate of random movement (diffusion) of organisms across the landscape and $f(u)$ is a function describing the population density at a particular time and place. This type of equation has been used to study critical patch size (Kierstead and Slobodkin 1953), biological invasions (Andro et al. 1990), and disease spread (Kallen et al. 1985). These models assume diffusion of organisms occurs over a homogeneous landscape (With 2002).

Realistically, landscapes are heterogeneous, requiring diffusion rates to vary with habitat type (Kareiva and Odell 1987). Fickian diffusion, of the form $\frac{\partial u}{\partial t} = \nabla[D(x_1, x_2)\nabla u]$, models the distribution of organisms along habitat quality or population density gradients (Holmes et al. 1994). It is derived from Fick's Law which states that the amount of substance that moves through a cross-section of the domain at time t is proportional to its density gradient ∇u (Logan 2006). For u representing a population, organisms move from high densities to low densities at a rate proportional to the density gradient, and are advected at a speed proportional to habitat gradients. This means that the organisms are making nonlocal decisions (i.e., sensing spatial differences in either habitat or population density) as they move (Turchin 1998).

Fickian diffusion has been used widely in ecological models (Kinezaki et al. 2003; Fitzgibbon et al. 2001; Lewis et al. 2005) and leads to a uniform population distribution at equilibrium, even when D varies spatially (Turchin 1998). That is, according to a Fickian model (and neglecting birth and death processes), organisms are just as likely to (eventually) be found in habitats that do not provide food and shelter as those which do, as well as on the boundaries of vastly different land cover types.

Although this may be appropriate for simple organisms at small scales, most animals do not diffuse like particles in heterogeneous environments (Okubo 1980). They are greatly influenced by habitat type, moving slowly through landscapes that provide needed resources and more quickly through inhospitable regions and are therefore much more likely to be found some places than others. Ecological diffusion, represented by $\frac{\partial u}{\partial t} = \nabla^2[\mu(x_1, x_2)u]$, accommodates this variation in motility, predicting that animals eventually accumulate in desirable habitats and leave or avoid undesirable ones (Turchin 1998). The motility parameter, μ, is analogous to the diffusion coefficient, D, in the Fickian diffusion equation, however, ecological diffusion gives an eventual distribution of animals which is inversely proportional to the motility. Ecological diffusion is appropriate when organisms make local decisions regarding movement, rather than nonlocal decisions as in the Fickian case, e.g., when their probability of moving or rate of movement depends entirely on the habitat within which they reside. Unlike Fickian diffusion, ecological diffusion supports discontinuous solutions, allowing for distinct population differences at habitat boundaries. A derivation of the ecological diffusion equation from a random walk is included in Turchin (1998), and is known as the Fokker–Planck or Kolmogorov equation without

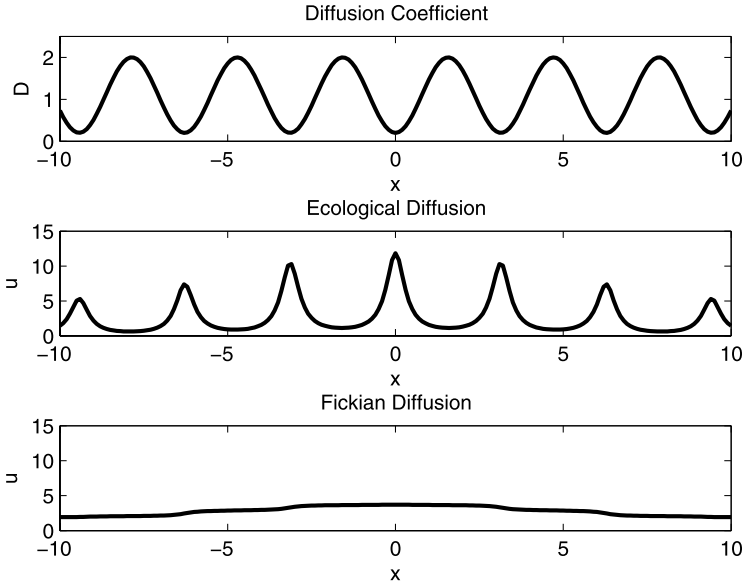

Fig. 1 A comparison of ecological diffusion with Fickian diffusion using the same diffusion (motility) coefficient and initial condition. After the same amount of time, the distribution of animals becomes inversely proportional to the motility with ecological diffusion, while becoming smooth over the entire domain with Fickian diffusion

an advection component (Risken 1986). A simple comparison of ecological diffusion with Fickian diffusion is shown in Fig. 1, illustrating the aggregation of individuals in areas with low motilities (longer residence times).

Although diffusion equations with variable coefficients reflect the heterogeneity of landscapes, they can be daunting to implement in a model, particularly at large spatial scales. A technique for facilely accommodating small scale variability in diffusion coefficients for large scale simulation is homogenization. Homogenization techniques for partial differential equations (PDEs) with Fickian diffusion have been widely used in engineering applications, such as heat transfer in composite materials, for decades. In ecology, they have been used in modeling such things as seed dispersal (Powell and Zimmermann 2004), the spread of biofilms (Demaret et al. 2009), the spread of feline leukemia (Fitzgibbon et al. 2001), and the relationship between dispersal ability and habitat fragmentation (Dewhirst and Lutscher 2009). The homogenization procedure, which uses the method of multiple scales (Holmes 1995), allows one to approximate PDEs that have rapidly-varying coefficients with similar 'homogenized' PDEs having averaged coefficients. The primary advantage is that the 'homogenized' PDE is framed in large scales in space and time, with the influence of the small scale variability in the averages.

Homogenized models are more efficient to solve numerically. Modeling the dispersal of organisms over a large area, such as the state of Utah, can be very computationally taxing, especially if the diffusion coefficient has variability on the scale of a meadow or stand of trees. Viewed from a suitably large spatial scale, however, many habitats have more or less periodic structure with repetitively interspersed subpatches

(Fitzgibbon et al. 2001). More generally, almost every landscape can be approximated as a section of a quasi-periodic function. This quasi-periodic structure allows us to use a homogenized PDE model to better understand a system at a large scale, while preserving the effects of fine scale variability in the diffusion coefficients. As far as we know, ecological diffusion, as defined above, has not been the subject of homogenization techniques; we will show that the homogenization technique and its effects are actually much simpler for ecological diffusion than Fickian diffusion.

Ecological diffusion and homogenization can be applied to spatial models in epidemiology. In particular, ecological diffusion is especially fitting for modeling wildlife diseases in free-ranging organisms, since the spread of a disease is linked to how hosts move and interact in a varying environment. A wildlife disease where such modeling efforts could be especially useful because of its potential impact to wildlife populations is chronic wasting disease (CWD). CWD is a contagious prion disease known to affect members of the Cervidae family which include deer (*Odocoileus* spp.), elk (*Cervus elaphus*), and moose (*Alces alces*) (Baeten et al. 2007). The disease is always fatal, and in mule deer (*Odocoileus hemionus*) infected animals can live from 12–24 months before outward signs of the disease become apparent (Williams 2005). Deer-to-deer and deer-to-environment interactions are important for transmission dynamics, and infectious prions can be shed into the environment from infected animals through feces, saliva and decaying carcasses where they may remain infective for many years (Miller et al. 2004; Johnson et al. 2006). It has been suggested that over decades CWD can affect local population dynamics with possible long-term effects on ecosystems (Miller et al. 2008).

CWD was first detected in free-ranging mule deer from Utah in 2002 and is currently found in three distinct geographic areas of the state (McFarlane 2007). The areas found in Utah represent movement of the disease west of the Rocky Mountains and delineate the western-most boundary for distribution of CWD in the United States. To predict the impact of CWD west of the Rockies, a compartmental model would be sufficient from a disease perspective, but would not capture the spatial aspects of spread. Current spatial disease models are constrained to spread a disease or population everywhere over the domain, using Fickian diffusion. Transmission of CWD is contingent on population densities which reflect the heterogeneity of the environment. In other words, density-dependent spatial spread is dependent on how patches of population at variable distances infect each other. This is not intuitive and requires a model incorporating ecological diffusion, to accommodate landscape variability. Here we develop a technique specifically designed to deal with spatial heterogeneity and apply it to a simple disease model. We are developing a more disease-specific CWD model with a coupled system of equations which will be the subject of a future paper. Even though the model will have increased complexity, ecological diffusion and our homogenization procedure will still apply.

To illustrate our homogenization technique we simulate the spread of CWD in mule deer in an area that includes the La Sal Mountains of Utah. Our homogenization technique introduces a way to numerically solve the model on a scale much larger (multiple kilometers) than the scale of variability (tens of meters) in the motility coefficients. Although variability in model parameters is reduced by the averaging, it

turns out that homogenization of ecological diffusion returns small scale variability to the result. This preservation of small-scale population consequences, coupled with the analytic simplicity, make homogenization of ecological diffusion a very attractive technique. As we will show, the computational time is markedly reduced, while the error introduced by the homogenization procedure is asymptotically small.

2 Model for CWD

To illustrate the idea of homogenizing ecological diffusion, let us consider a simple spatial model for CWD in mule deer based on a general model for a disease with no recovery. What sets this model apart from other spatial epidemiology models is the use of ecological diffusion rather than diffusion with a constant coefficient as in Meade and Milner (1992).

We will assume that the disease is in its initial stage, spread by direct contact of diseased individuals with healthy individuals, and always fatal. Mule deer in Utah are a managed game species, with population estimates projected using computer models. We therefore assume death from causes other than CWD is balanced by births, and we will ignore the environmental hazard associated with CWD (which is the subject of ongoing research). Similarly, we will ignore other modeling considerations such as seasonal and sex differences in movement and age structure of the disease for purposes of developing the homogenization approach. Uninfected and infected individuals are linked as in a traditional SI model,

$$S_t = \nabla^2(\mu S) - \beta SI, \tag{1}$$

and

$$I_t = \nabla^2(\mu I) + \beta SI - \lambda I, \tag{2}$$

where S refers to the susceptible population and I refers to the infected population. The differential operator,∇^2, is the Laplacian, $\frac{\partial^2}{\partial {x_1}^2} + \frac{\partial^2}{\partial {x_2}^2}$, and the parameter, $\mu = \mu(x_1, x_2)$, is the spatially varying motility coefficient. The infection rate, β, and the rate of death from the disease, λ, may also vary spatially if behaviors are linked to habitat type. The motility, which is inversely proportional to residence time, will be low in areas where the deer linger for food and shelter, and high in the places devoid of resources (Turchin 1998).

In the initial stages of the spread of a disease, it is appropriate to view the healthy population as predominant. When the number of infected deer is very small compared to susceptibles, $0 < I \ll S$, and (1) becomes $S_t = \nabla^2(\mu S)$, which has the steady-state solution

$$\tilde{S} = \frac{K}{\mu}, \tag{3}$$

where K is a constant proportional to the total number of susceptible individuals. Then the initial spread of the disease is captured by

$$I_t = \nabla^2\big[\mu(\boldsymbol{x})I\big] + \beta\tilde{S}I - \lambda I = \nabla^2\big[\mu(\boldsymbol{x})I\big] + \alpha(\boldsymbol{x})I, \tag{4}$$

where $\alpha(x) = \beta\tilde{S} - \lambda = \beta\frac{K}{\mu(x)} - \lambda$ varies spatially as $\tilde{S}$ varies over the landscape. The model given in (4) is very general, applying to all manner of spatial invasion and dispersal situations, except using ecological diffusion.

3 Homogenization of a Model with Ecological Diffusion

In order for (4) to reflect the connection of the spread of CWD with the movement of deer, we need to know the habitat types comprising the desired landscape and estimate a motility value for each type. The National Land Cover Database (NLCD) provided by U.S. Geological Survey Landcover Institute classifies habitat in 30×30 meter blocks (Homer et al. 2007). If we assume those blocks form a repeating pattern over a much larger scale, say 9×9 kilometer blocks, we can regard μ as varying quickly over the small scale and much more slowly over the large scale. Viewing μ in (4) as varying over two different scales in this manner allows us to apply a homogenization procedure similar to the one derived for two-dimensional Fickian diffusion in Holmes (1995). However, as we will show, the result for ecological diffusion is much simpler and easier to use in computer simulations. The homogenization procedure for the one spatial dimension case is derived in Hooten et al. (2009).

The easiest way to apply the homogenization procedure is to assume a quasi-periodic motility function, which allows the periodicity to vary on the large scale. We will discuss this assumption in detail in the periodicity assumption section below, showing that this assumption is much more broad then might be expected. Let the order parameter, ϵ, represent the ratio of small and large scales; for the landscape described above, $\epsilon = \frac{30}{9000} = \frac{1}{300}$. Let $\boldsymbol{x}$ be the large spatial scale in two spatial dimensions, with an associated slow time scale, t. Then the small scale $\boldsymbol{y}$ is defined in relation to $\boldsymbol{x}$ by $\boldsymbol{y} = \frac{\boldsymbol{x}}{\epsilon}$. Thus $O(\epsilon)$ changes in $\boldsymbol{x}$ become $O(1)$ changes in $\boldsymbol{y}$ (Powell and Zimmermann 2004). The fast time scale associated with $\boldsymbol{y}$ is $\tau = \frac{t}{\epsilon^2}$. The motility coefficient thus becomes a function of both spatial scales, $\mu = \mu(\boldsymbol{x}, \boldsymbol{y})$. Quasi-periodicity means that there exits a vector $\boldsymbol{p}(\boldsymbol{x})$ such that

$$\mu\big(\boldsymbol{x}, \boldsymbol{y} + \boldsymbol{p}(\boldsymbol{x})\big) = \mu(\boldsymbol{x}, \boldsymbol{y}) \tag{5}$$

for all $\boldsymbol{x}$ and $\boldsymbol{y}$ under consideration.

3.1 Derivation of Homogenized Model

We now employ the method of multiple scales. The derivatives transform, with $\nabla \longrightarrow \nabla_x + \frac{1}{\epsilon}\nabla_y$, where the subscript indicates the variable being differentiated, and $\frac{\partial}{\partial t} \longrightarrow \frac{1}{\epsilon^2}\frac{\partial}{\partial \tau} + \frac{\partial}{\partial t} = \frac{1}{\epsilon^2}\partial_\tau + \partial_t$. Substituting the new scales and derivatives into (4) gives (after multiplication by ϵ^2)

$$\big(\partial_\tau + \epsilon^2\partial_t\big)I = (\nabla_y + \epsilon\nabla_x) \cdot \big[(\nabla_y + \epsilon\nabla_x)\mu(\boldsymbol{x}, \boldsymbol{y})I\big] + \epsilon^2\alpha I. \tag{6}$$

The dependent variable, I, is now a function of t, τ, $\boldsymbol{x}$, and $\boldsymbol{y}$. We replace I in (6) with a power expansion in ϵ,

$$I = I_0(\boldsymbol{x}, \boldsymbol{y}, t, \tau) + \epsilon I_1(\boldsymbol{x}, \boldsymbol{y}, t, \tau) + \epsilon^2 I_2(\boldsymbol{x}, \boldsymbol{y}, t, \tau) + O\big(\epsilon^3\big), \tag{7}$$

and gather terms of common powers of ϵ.

At $O(1)$ this gives

$$\partial_\tau I_0 = \nabla_y{}^2(\mu I_0). \tag{8}$$

Since the term on the left hand side of (8) involves a derivative in the fast time scale, τ, and the equation is parabolic, the solution decays rapidly to its steady state. In fact, the transient parts of the solution decay to zero as $\epsilon \to 0$ like $e^{-\frac{\mu_1 t}{L^2\epsilon^2}}$, where μ_1 is a lower bound on μ, i.e., $0 < \mu_1 < \mu$, and L^2 is the area of the largest habitat patch. Since $e^{-\frac{\mu_1 t}{L^2\epsilon^2}} \ll \epsilon$ for all $t > 0$, we neglect transients and solve

$$\nabla_y{}^2(\mu I_0) = 0. \tag{9}$$

A solution for (9) (using periodicity in $\boldsymbol{y}$) is

$$I_0 = \frac{c(\boldsymbol{x}, t)}{\mu(\boldsymbol{x}, \boldsymbol{y})}, \tag{10}$$

with $c = c(\boldsymbol{x}, t)$ having no $\boldsymbol{y}$ dependence.

The $O(\epsilon)$ equation is

$$\partial_\tau I_1 = \nabla_y{}^2(\mu I_1) + \nabla_x \cdot \left[\nabla_y(\mu I_0)\right] + \nabla_y \cdot \left[\nabla_x(\mu I_0)\right]. \tag{11}$$

Substituting (10) into (11) and simplifying (noting that $\nabla_y \cdot (\mu I_0) = \nabla_y c(\boldsymbol{x}, t) = 0$), we have

$$\partial_\tau I_1 = \nabla_y{}^2(\mu I_1). \tag{12}$$

Considering the steady state problem as in the $O(\epsilon^0)$ case, the solution is of the form

$$I_1 = \frac{b(\boldsymbol{x}, t)}{\mu}. \tag{13}$$

Due to homogeneous boundary conditions for all orders above ϵ^0, we deduce $I_1 = 0$.

The $O(\epsilon^2)$ equation is

$$\partial_\tau I_2 + \partial_t I_0 = \nabla_y{}^2(\mu I_2) + \nabla_x{}^2(\mu I_0) + \alpha I_0. \tag{14}$$

Substituting (10) into (14) and considering again the steady state with respect to the fast time scale (i.e., $\partial_\tau I_2 = 0$) yields

$$\partial_t\left(\frac{c}{\mu}\right) = \nabla_y{}^2(\mu I_2) + \nabla_x{}^2 c + \alpha\frac{c}{\mu}. \tag{15}$$

Let $\boldsymbol{p}(\boldsymbol{x})$ in (5) be defined as the periodicity vector $\boldsymbol{p}(\boldsymbol{x}) = [l_1(x_1), l_2(x_2)]^T$. We determine the homogenized problem by averaging each term of (15) over a $l_1(x_1) \times l_2(x_2)$ cell, with area $A = l_1(x_1)l_2(x_2)$, following Holmes (1995). The average of a function $v(\boldsymbol{x}, \boldsymbol{y})$ over an $l_1(x_1) \times l_2(x_2)$ cell is defined as

$$\langle v \rangle = \frac{1}{A}\int_0^{l_1(x_1)}\int_0^{l_2(x_2)} v(\boldsymbol{x}, \boldsymbol{y})\, dy_1\, dy_2. \tag{16}$$

Note that this is not the average value of the function over the entire domain. It is a local average for the current position of interest, and the region of integration depends on the (changing) local cell size.

Using the Divergence Theorem and periodicity on a cell,

$$\langle {\nabla_y}^2(\mu I_2)\rangle = \frac{1}{A}\int_{\partial\Omega_0} \boldsymbol{n}\cdot\nabla_y(\mu I_2)\,dS_y = 0, \tag{17}$$

where $\partial\Omega_0$ is the boundary of the cell, $\boldsymbol{n}$ is the outward normal vector, and dS_y is along the cell boundary. This is valid if we require $\lim_{x\uparrow x_0}(\mu_1 I) = \lim_{x\downarrow x_0}(\mu_2 I)$ and $\lim_{x\uparrow x_0}[\nabla(\mu_1 I)\cdot\boldsymbol{n}] = \lim_{x\downarrow x_0}[\nabla(\mu_2 I)\cdot\boldsymbol{n}]$ where μ_1 and μ_2 are the values of μ for two adjacent cells, x_0 is the location of their shared boundary. This means that on the boundary of cells with different motilities, the number of infected individuals that are mobile is proportional to μI. The flux of individuals over the boundary is proportional to the first derivative of μI (as opposed to μ times the derivative of I), which is a consequence of using ecological diffusion. Thus, the density of the infected population over the landscape reflects the habitat boundaries defined by the motility coefficients at the resolution of the land cover data.

Averaging the other terms in (15) yields

$$\left\langle \partial_t\left(\frac{c}{\mu}\right)\right\rangle = \langle\mu^{-1}\rangle\partial_t c \tag{18}$$

and

$$\left\langle \alpha\frac{c}{\mu}\right\rangle = \left\langle\frac{\alpha}{\mu}\right\rangle c. \tag{19}$$

The term ${\nabla_x}^2 c$, which has no $\boldsymbol{y}$ dependence, remains unchanged by the averaging procedure.

Equation (15) is now homogenized,

$$\langle\mu^{-1}\rangle\partial_t c = {\nabla_x}^2 c + \left\langle\frac{\alpha}{\mu}\right\rangle c, \tag{20}$$

where

$$\langle\mu^{-1}\rangle = \frac{1}{A}\int_0^{l_1(x_1)}\int_0^{l_2(x_2)}\frac{1}{\mu}\,dy_1\,dy_2 \tag{21}$$

and

$$\left\langle\frac{\alpha}{\mu}\right\rangle = \frac{1}{A}\int_0^{l_1(x_1)}\int_0^{l_2(x_2)}\frac{\alpha}{\mu}\,dy_1\,dy_2. \tag{22}$$

Simplifying we can write (20) as

$$\partial_t c = \bar{\mu}{\nabla_x}^2 c + \bar{\mu}\left\langle\frac{\alpha}{\mu}\right\rangle c, \tag{23}$$

where $\bar{\mu} = \frac{1}{\langle\mu^{-1}\rangle}$ is the harmonic average of $\mu(\boldsymbol{x},\boldsymbol{y})$ over an $l_1(x_1)\times l_2(x_2)$ cell. Our homogenized equation (23) is now in terms of the large spatial scale $\boldsymbol{x}$ and the slow

time scale t. The small scale variability, however, still influences the leading order solution for infectives through the averages and through the definition of $c(\boldsymbol{x}, t)$. The function $c = c(\boldsymbol{x}, t)$, which is a function of the long time scale and the large spatial scale, relates to the leading order distribution of diseased animals by

$$I_0 = \frac{c(\boldsymbol{x}, t)}{\mu(\boldsymbol{x}, \boldsymbol{y})}. \tag{24}$$

Thus the homogenized solution reflects small scale variability (as it should), but can be solved dynamically on large time/space scales. The multiple-scale approach makes sense in the context of the spread of CWD. The spread of the disease is closely related to the movement of deer, which stabilizes rapidly on the timescale of τ, but can be viewed as stationary on the long time scale, t. Therefore, changes in the population distribution over the landscape occur on a scale of hours or days, while changes in the disease dynamics occur over years. Spatially, local movement and interaction of deer underly the large-scale spread of CWD. This homogenization technique can be applied to more complex disease or invasion models as will be illustrated in a future paper.

The result of homogenizing ecological diffusion is surprisingly simple when compared to the homogenization of Fickian diffusion as derived in Holmes (1995). In the Fickian case, the large-scale diffusion coefficient is not simply a harmonic mean but rather a matrix of averages depending on solutions to an associated elliptic PDE on a cell. The ecological diffusion result also differs from the Fickian case in that the small scale variability is still present in the solution due to its inverse proportionality to μ. This is an unexpected benefit of applying the method of multiple scales to ecological diffusion. Fickian diffusion loses ecologically realistic small-scale behavior under homogenization, but this behavior is preserved by homogenization of ecological diffusion.

Although the presence of the harmonic average of μ in the homogenized equation (23) is a natural result of the homogenization process, it also intuitively makes sense. As mentioned in the introduction, if μ is constant in a contiguous block, it is inversely proportional to the mean residence time in that block (Turchin 1998). Given a large landscape unit containing $n_1, n_2, \ldots, n_k$ number of blocks with corresponding areas $A_1, A_2, \ldots, A_k$ and motilities $\mu_1, \mu_2, \ldots, \mu_k$, the projected residence time, T, for individuals in the unit would be

$$T = \frac{n_1 A_1}{\mu_1} + \frac{n_2 A_2}{\mu_2} + \cdots + \frac{n_k A_k}{\mu_k}, \tag{25}$$

since $\frac{A_i}{\mu_i}, i = 1, \ldots, k$, is the mean residence time of each individual block. Then the effective μ for the entire unit, which we will call $\bar{\mu}$ becomes,

$$\bar{\mu} = \frac{n_1 A_1 + n_2 A_2 + \cdots + n_k A_k}{T} = \frac{n_1 A_1 + n_2 A_2 + \cdots + n_k A_k}{\frac{n_1 A_1}{\mu_1} + \frac{n_2 A_2}{\mu_2} + \cdots + \frac{n_k A_k}{\mu_k}}, \tag{26}$$

where $n_1 A_1 + n_2 A_2 + \cdots + n_k A_k$ is the total area of the unit. Noting

$$\frac{n_1 A_1}{\mu_1} + \frac{n_2 A_2}{\mu_2} + \cdots + \frac{n_k A_k}{\mu_k} = (n_1 A_1 + n_2 A_2 + \cdots + n_k A_k)\left\langle \frac{1}{\mu} \right\rangle, \tag{27}$$

and substituting into (26), we see

$$\bar{\mu} = \frac{1}{\langle \frac{1}{\mu} \rangle}, \tag{28}$$

which is the harmonic mean of μ.

The average $\bar{\mu}\langle \frac{\alpha}{\mu} \rangle$ also has an intuitive meaning. If $\alpha_1, \alpha_2, \ldots, \alpha_k$ are the net rates of change in the population density of infected deer in the corresponding blocks, $n_i A_i$, of motility μ_i, then

$$\left\langle \frac{\alpha}{\mu} \right\rangle = \frac{n_1\alpha_1 \frac{A_1}{\mu_1} + n_2\alpha_2 \frac{A_2}{\mu_2} + \cdots + n_k\alpha_k \frac{A_k}{\mu_k}}{n_1 A_1 + n_2 A_2 + \cdots + n_k A_k}. \tag{29}$$

Using (26) and simplifying,

$$\begin{aligned} \bar{\mu}\left\langle \frac{\alpha}{\mu} \right\rangle &= \frac{n_1\alpha_1 \frac{A_1}{\mu_1} + n_2\alpha_2 \frac{A_2}{\mu_2} + \cdots + n_k\alpha_k \frac{A_k}{\mu_k}}{n_1 \frac{A_1}{\mu_1} + n_2 \frac{A_2}{\mu_2} + \cdots + n_k \frac{A_k}{\mu_k}} \\ &= \frac{n_1\alpha_1 \frac{A_1}{\mu_1} + n_2\alpha_2 \frac{A_2}{\mu_2} + \cdots + n_k\alpha_k \frac{A_k}{\mu_k}}{T}. \end{aligned} \tag{30}$$

The denominator is the expected residence time, T, from (25). Rewriting (30) with $t_i = \frac{A_i}{\mu_i}$ as the mean residence time for each block, we have

$$\bar{\mu}\left\langle \frac{\alpha}{\mu} \right\rangle = \frac{n_1\alpha_1 t_1 + n_2\alpha_2 t_2 + \cdots + n_k\alpha_k t_k}{T}. \tag{31}$$

If we consider (23) without the diffusion term, the solution for $c_t = \bar{\mu}\langle \frac{\alpha}{\mu} \rangle c$ is the projected increase or decrease in the density of infected deer due to the time spent in the unit. It is of the form

$$c = \underbrace{e^{\alpha_1 \frac{t_1}{T} t} e^{\alpha_1 \frac{t_1}{T} t} \cdots e^{\alpha_1 \frac{t_1}{T} t}}_{n_1 \text{times}} \underbrace{e^{\alpha_2 \frac{t_2}{T} t} e^{\alpha_2 \frac{t_2}{T} t} \cdots e^{\alpha_2 \frac{t_2}{T} t}}_{n_2 \text{times}} \cdots \underbrace{e^{\alpha_k \frac{t_k}{T} t} e^{\alpha_k \frac{t_k}{T} t} \cdots e^{\alpha_k \frac{t_k}{T} t}}_{n_k \text{times}} \tag{32}$$

$$= (e^{n_1\alpha_1 t_1} e^{n_2\alpha_2 t_2} \cdots e^{n_k\alpha_k t_k})^{\frac{t}{T}} = e^{\frac{\sum_{i=1}^{k} n_i\alpha_i t_i}{T} t} = e^{\bar{\mu}\langle \frac{\alpha}{\mu} \rangle t}, \tag{33}$$

where α_i is the net rate of change in the density of infected deer and $\frac{t_i}{T}$ is the fraction of time spent in the habitat with area A_i and motility μ_i, and t is the time spent in the unit. Noting $c_t = \bar{\mu}\langle \frac{\alpha}{\mu} \rangle c$, we see that (31) is the projected exponential rate of change. So the average $\bar{\mu}\langle \frac{\alpha}{\mu} \rangle$ can be thought of as the net effect of the rates of contracting the disease in different habitats depending on the time spent in each habitat.

A one-dimensional example of solutions to this homogenized model is shown in Fig. 2. Figure 2(c) compares the solutions for the non homogenized model ((3) and (4)) and the homogenized model ((23) and (24)) with a continuous $\mu(x, y = \frac{x}{\epsilon})$, shown in Fig. 2(a). The solution illustrates the idea that the population density of diseased animals will be greater in areas of low motility and less in areas of high motility.

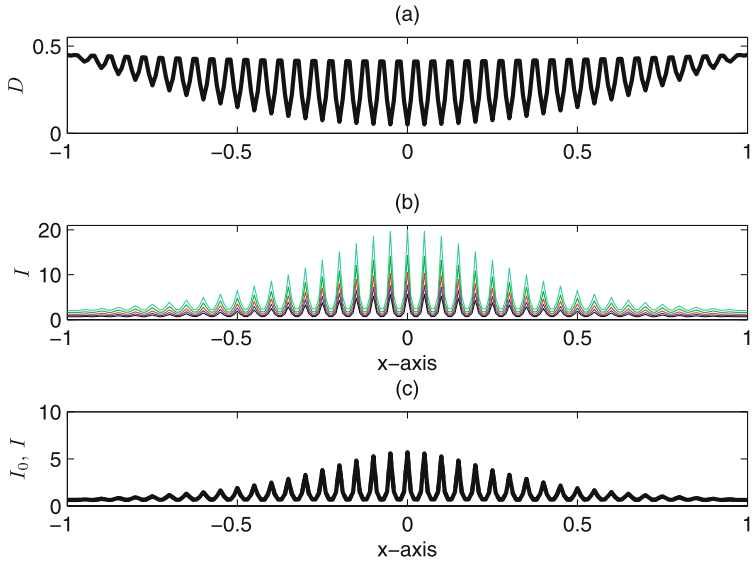

Fig. 2 Graph (**a**) shows a one-dimensional example of a continuous $\mu(x, y = \frac{x}{\epsilon})$ with an obvious relationship between the large and small scales. $\mu(x, y) = 0.45 - 0.2(1 - x^2)(1 + \cos(2\pi y))$, with $\epsilon = 0.05$. The time evolution of solution is shown in graph (**b**). The *lightest shade* is the initial condition, with subsequent times becoming *darker*. The solutions, I for the non-homogenized model and I_0 for the leading order distribution of sick animals, are plotted on top of each other in graph (**c**). The difference between I and I_0 is not visually apparent with the maximum error, $\max(|I - I_0|) = 0.027$

3.2 Periodicity Assumption

The homogenization procedure we have just described is facilitated by a quasi-periodicity assumption on the motility coefficient. We want to apply this procedure to natural landscapes that are not periodic in the strict sense, but also not completely random. Here we wish to argue that the assumption of quasi-periodicity applies broadly, and in particular to natural landscapes. When viewed at large scales there are repeating elements such as mountains and valleys or subpatches of different habitat types. We apply this procedure to landscapes by allowing the periodicity to vary with the slow variable $\boldsymbol{x}$ (Holmes 1995), as in (5).

To illustrate this idea in one dimension, consider functions, $f(x)$, which have Fourier transforms of the form

$$\hat{f} = \frac{1}{\epsilon}\hat{g}\left(\frac{k - k_0}{\epsilon}\right) + \text{ c.c.}, \tag{34}$$

where c.c. denotes the complex conjugate. The graph of $|\hat{f}|^2$ has a peak at k_0, indicating repeating elements at a scale of $\frac{2\pi}{k_0}$.

The inverse Fourier transform for $f(x)$ is

$$2\pi f(x) = \int_{-\infty}^{\infty} \frac{1}{\epsilon}\hat{g}\left(\frac{k - k_0}{\epsilon}\right) e^{iky}\, dk + \text{ c.c.} \tag{35}$$

Let $l = \frac{k-k_0}{\epsilon}$. Then $k = k_0 + \epsilon l$, $dk = \epsilon\, dl$, and (35) becomes

$$2\pi f(x) = \int_{-\infty}^{\infty} \frac{1}{\epsilon} \hat{g}(l) e^{i(k_0+\epsilon l)y} \epsilon\, dl + \text{ c.c.} = e^{ik_0 y} \int_{-\infty}^{\infty} \hat{g}(l) e^{il(\epsilon y)}\, dl + \text{c.c.} \quad (36)$$

Noting $x = \epsilon y$ gives

$$f(x) = e^{ik_0 y} g(x = \epsilon y) + \text{ c.c.}, \quad (37)$$

where $e^{ik_0 y}$ is the carrier wave and $g(x)$ is a slowly-varying envelope function.

Writing $g(x)$ in polar coordinates, $g(x) = h(x)e^{im(x)x}$, where m and h are both real. Then

$$f(x) = h(x)e^{i(k_0 y + m(x)x)} + \text{ c.c.} = h(x)e^{iy(k_0+\epsilon m(x))} + \text{ c.c.}, \quad (38)$$

using $x = \epsilon y$. Therefore, $f(x)$ is periodic with the period $p(x) = \frac{2\pi}{k_0+\epsilon m(x)}$ which varies in the slow variable x.

Thus, functions with clear, narrow peaks in their spectrum can naturally be viewed as quasi-periodic. While this is no guarantee that a given motility distribution will be quasi-periodic, all of the landscape that we have classified using deer motilities in Utah had precisely this Fourier structure, possibly due to interactions between the 30×30 meter landscape classification and natural periodicities of the landscape. In any event, we now assume that the landscape of interest can be viewed as periodic in the fast scale with slowly varying periodic function, $\boldsymbol{p}(\boldsymbol{x})$. Now the challenge is that we do not know $\boldsymbol{p}(\boldsymbol{x})$ precisely, and the homogenization procedure outlined above requires exact knowledge of $\boldsymbol{p} = [l_1(x_1), l_2(x_2)]$. We now address this difficulty.

If we divide the landscape into rectangular regions for the averaging procedure, we can view each region as a multiple of the quasi-periodicity function $\boldsymbol{p}(\boldsymbol{x}) = [l_1(x_1), l_2(x_2)]^T$ plus a small remainder. Let R^* be the chosen rectangular region with area A_{R^*} that contains a region R with area $A_R = Nl_1(x_1)Ml_2(x_2)$, where NM is the largest multiple of an $l_1(x_1)l_2(x_2)$ cell that fits into R^*. Then the region $R^* - R$ is the small remainder with area A_{R^*-R} (see Fig. 3). Let f be a motility function with periodicity as defined in (5). Then using the average defined in (16)

$$\langle f \rangle = \frac{1}{Nl_1 Ml_2} \int_0^{Nl_1(x_1)} \int_0^{Ml_2(x_2)} f(\boldsymbol{x}, \boldsymbol{y})\, dy_1\, dy_2 = \frac{1}{A_R} \int_R f\, dA \quad (39)$$

$$= \frac{1}{A_R} \left[\int_R f\, dA + \int_{R^*-R} f\, dA - \int_{R^*-R} f\, dA \right] \quad (40)$$

$$= \frac{A_{R^*}}{A_R} \langle f \rangle_{R^*} - \frac{1}{A_R} \int_{R^*-R} f\, dA. \quad (41)$$

So,

$$\langle f \rangle_{R^*} = \frac{A_R}{A_{R^*}} \langle f \rangle + \frac{1}{A_{R^*}} \int_{R^*-R} f\, dA. \quad (42)$$

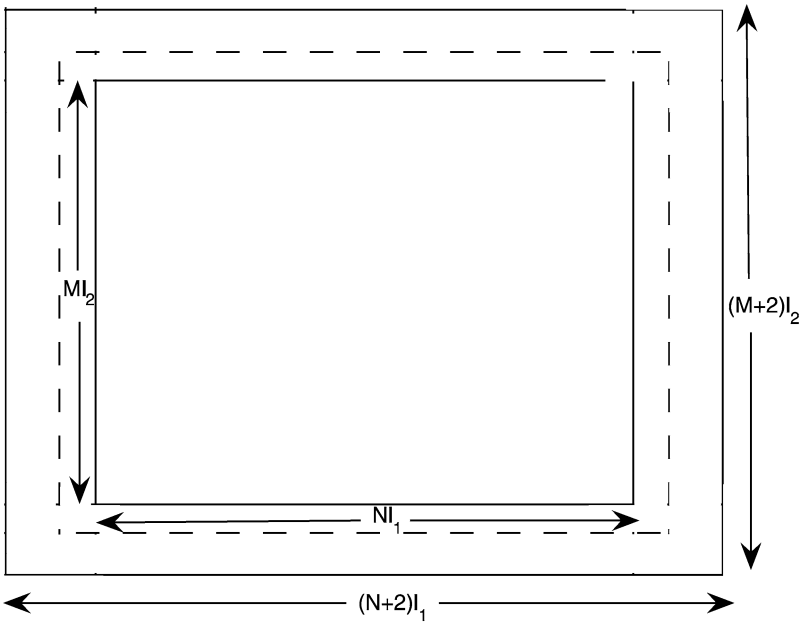

Fig. 3 An illustration of choosing a *rectangle* to average over without knowing $\boldsymbol{p}(\boldsymbol{x})$ explicitly. The region enclosed in the *dashed line* is R^*. The *smallest rectangle* is the region R with area $Nl_1 Ml_2$

Since R is a smaller region than R^*, $\frac{A_R}{A_{R^*}} < 1$ and the second term in (42) can be bounded by

$$\left| \frac{1}{A_{R^*}} \int_{R^*-R} f \, dA \right| < \frac{[2l_1 l_2(N+1) + 2l_1 l_2(M+1)]|f|_{\max}}{l_1 l_2 NM} = \frac{2(M+N+2)|f|_{\max}}{NM}, \tag{43}$$

resulting in

$$\langle f \rangle_{R^*} < \langle f \rangle + \frac{2(M+N+2)|f|_{\max}}{NM}. \tag{44}$$

If we choose N and a corresponding M such that

$$\frac{2(M+N+2)|f|_{\max}}{NM} < \epsilon, \tag{45}$$

then

$$\langle f \rangle_{R^*} = \langle f \rangle + O(\epsilon). \tag{46}$$

Thus, the lack of explicit knowledge concerning $\boldsymbol{p}(\boldsymbol{x})$ does not influence the homogenization at leading order if we replace $\langle \mu \rangle$ with $\langle \mu \rangle_{R^*}$, since the introduced error is $O(\epsilon)$.

4 A Two-Dimensional Example

To illustrate our homogenization result, we apply the simple model, (3) and (4), and the homogenized model, (23) and (24), to the spread of CWD in a 26.1×33.36 kilometer piece of mule deer habitat in the La Sal mountains of Utah. Land cover types comprising the area were determined using the National Land Cover Database (Homer et al. 2007). Motility coefficients (μ) were estimated from GPS movement data for collared deer collected by the Utah Division of Wildlife Resources (McFarlane 2007). This was done by parsing the movement data by habitat type, then estimating the mean-squared displacement per time for all movements within each habitat (Turchin 1998); these efforts will be discussed in more detail in a future paper. Motility values for the different habitat types in the area are illustrated in Fig. 4 and given in Table 1. The habitat types for the inset in Fig. 4 are shown in detail in Fig. 5. We used an initial population of 7400 deer for the entire area and a small distribution of infected deer (equivalent to approximately 38 deer) in the eastern part of the mountains where the disease was first found (U.D.W.R. 2010). We used the infection rate, $\beta = 0.0326\ \text{yr}^{-1}\ \text{density}^{-1}$, and the death rate from CWD, $\lambda = 0.481\ \text{yr}^{-1}$, found in Miller et al. (2006) and converted to units of days^{-1}.

An alternating direction implicit (ADI) numerical method with no-flux boundaries was used to compute the population density of infected deer over time for both the homogenized and non-homogenized models. ADI is an implicit finite difference method which splits each time step into two stages, a discretization in the x_1 direction, followed by a discretization in the x_2 direction (Mitchell and Griffiths 1980). This is equivalent to solving two tridiagonal systems for each time step. The details

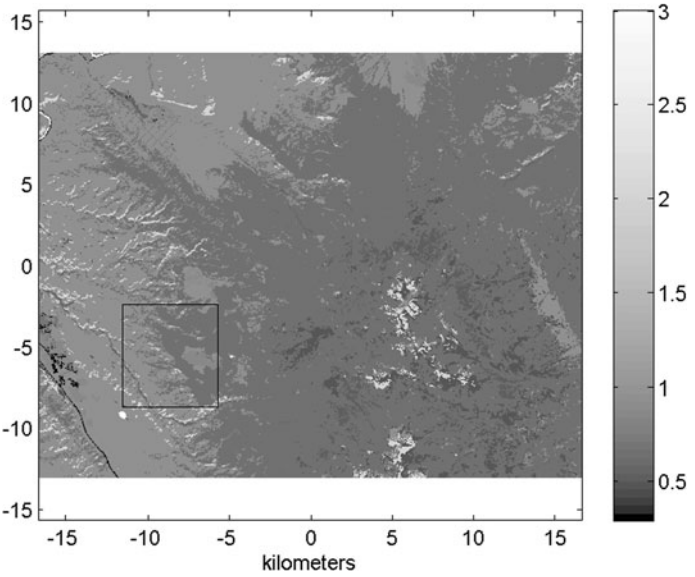

Fig. 4 The assigned motility values for the habitat types of mule deer habitat in the La Sal mountains of Utah. *Light shades* indicate areas of high motility and *darker shades* indicate areas of low motility. A closer view of the outlined portion is shown in Fig. 5

Table 1 The estimated motility values (μ) for the land cover types used in the two-dimensional example

Land cover type	Estimated μ ($\frac{km^2}{day}$)
Rock	2.01
Scrub	0.97
Conifer forest	0.66
Deciduous forest	0.65
Mixed forest	0.52
Pasture	0.85
Cultivated crops	0.86
Grassland	0.51
Developed (low intensity)	0.29
Developed (medium intensity)	0.30
Developed (open space)	0.70
Woody wetlands	0.55
Open water	3.02

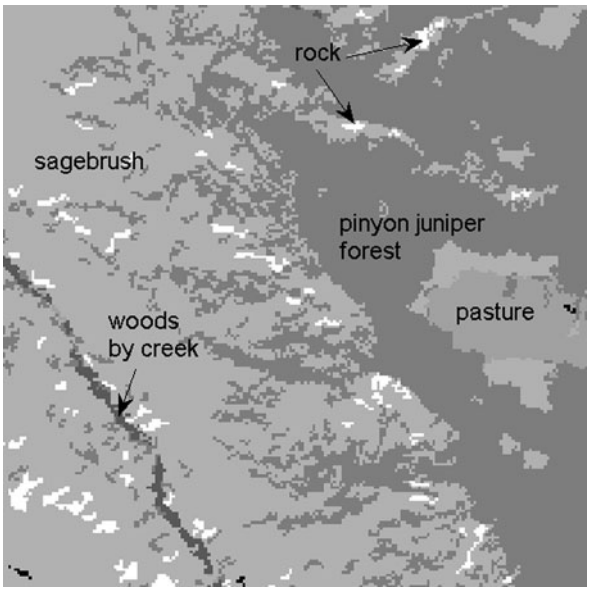

Fig. 5 The assigned motility values for the habitat types in the outlined portion of Fig. 4. The high motilities represent areas such as barren rock formations (where deer are absent) and sagebrush areas where deer spend a great amount of time moving (*light shades*). The low motilities represent areas where the residence time is high such as in pinyon juniper, deciduous, or mixed forest habitats where they bed and ruminate during daylight hours (*dark shades*)

of this method are included in the Appendix. We chose an ADI method for its ease in accommodating the variable motility coefficient, as well as its efficiency and stability.

For the non-homogenized model (4), we chose a computational grid that aligned with the 30×30 meter land cover type blocks. For the homogenized model (23) and (24), we chose $\epsilon = 0.01$ which corresponds to averaging over 3000×3000 meter blocks. The technique is also valid for other choices of $\epsilon \ll 1$. We used a computational grid of 600×600 meter blocks for the numerical solution of the homogenized model, with each computational grid point being the center of a 3000×3000 meter block used for averaging. The periodicity assumption was used to provide μ values

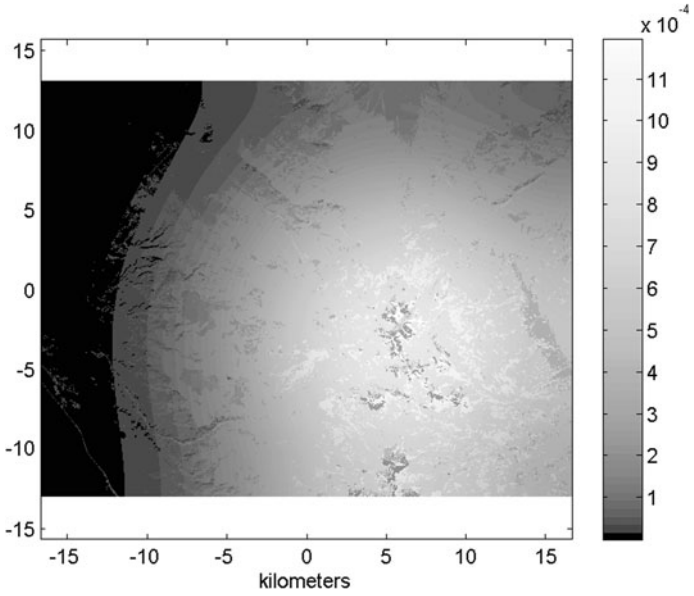

Fig. 6 A view of the values for the population densities for infected deer for the homogenized model. The idea that animals collect in areas with low motilities is illustrated when compared with the motility values in Fig. 4

for a grid larger than the study area for computing averages at grid points on the boundary. This choice resulted in a significant reduction in the number of needed operations as compared with solutions for the non-homogenization model. The non-homogenized model with n spatial steps in each direction and m time steps takes $O(mn^2)$ operations. If δ is the ratio of the large scale spatial steps to small scale spatial steps ($\delta = 0.05$ in our example), then the homogenized model with δn spatial steps in each direction with δm time steps takes $O(\delta^3 mn^2)$ operations. In terms of time saved for this example, the non-homogenized model took 45 hours, 6 minutes and 11.51 seconds to run for 365 days, compared to 3.85 seconds for the homogenized model. That is $\frac{1}{42000}$ of the time, a substantial computational savings.

The results of the two-dimensional example are shown in Figs. 6 and 7. Figure 6 shows the population densities for infected deer after 1 year for the homogenized model. Solving (23) for the intermediate variable c resulted in the infection being spread over the landscape at the diffusion rate of the averaged motilities $\bar{\mu}$. The density of infected deer is then prorated by division by μ in (24). This places disease hotspots in the habitat types where deer naturally gather, such as forests and riparian areas. As expected, the model predicts low densities of infected animals in areas of high motility, such as rocky, barren areas and developed open space. A comparison of the homogenized and non-homogenized models is shown in Fig. 7. The maximum error between the homogenized and non-homogenized models is consistently $O(\epsilon)$. The surfaces in this figure are not smooth, but reflect the effect of motility on the density of infected deer.

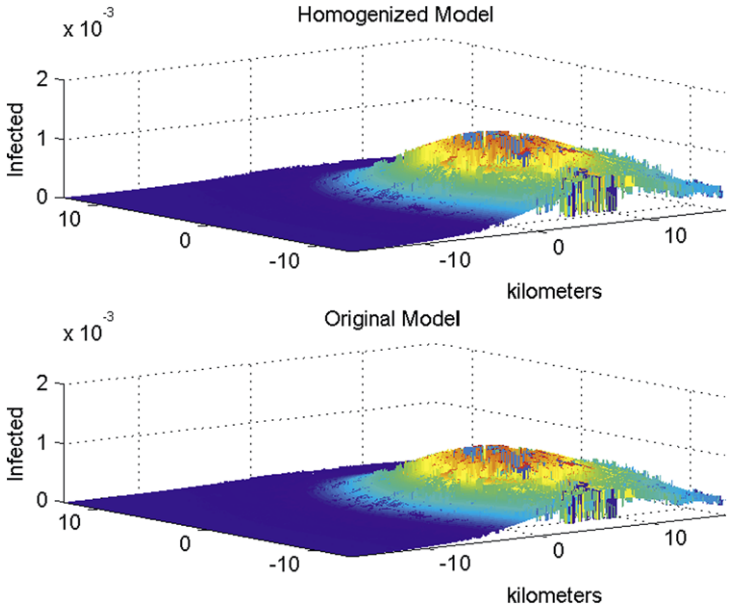

Fig. 7 This figure shows results from running the homogenized model with $\epsilon = 0.01$ and the original model. The maximum error between the two models was 1.86×10^{-4}. An initial condition representing a small density of diseased deer in the eastern part of the region was used. This graph represents the spread of the disease over a year in the 26.1×33.36 kilometer study area

5 Discussion

When modeling population densities of animals over a heterogeneous environment, ecological diffusion, $\nabla^2[\mu(x_1, x_2)u]$, allows for the accumulation of animals in habitats where they linger and not in areas they naturally avoid. Fickian diffusion, $\nabla[D(x_1, x_2)\nabla u]$, gives a smooth distribution of animals over the landscape, disregarding the underlying motility.

The model used in this paper is a general model for the spread of a disease, using ecological diffusion. It is meant to illustrate the appropriateness of ecological diffusion in the context of heterogeneous landscapes and to demonstrate our homogenization procedure. We are developing a more disease specific CWD model, which will be the subject of a future paper. Contact with disease agents in the environment as well as contact between susceptible and infected individuals will be considered. The behavioral differences of male and female deer during the seasons of the year will be incorporated to more effectively model disease dynamics. Female deer form matrilineal groups with fidelity to summer and winter ranges while male deer wander between groups, especially during breeding season (McFarlane 2007). The estimation of motility values for male and female deer from GPS movement data using Bayesian methods will be explored. Harvesting and culling practices for the study area will be modeled as well.

This will result in a system consisting of separate equations for males and females in both susceptible and infected classes and an equation for environmental hazard.

How behavioral differences between males and females affect disease spread can be explored through various infection rates. The environmental impact of diseased females vs males can also be explored.

Another management application of this model is determining a critical population of deer for which the wave speed of the spread of CWD is zero, that is, is the wavefront speed in this area sufficient to allow the disease to propagate? The wave speed, v, for solutions to the homogenized PDE, can be determined for an area of interest by $v \approx 2\sqrt{\bar{\mu}\bar{\alpha}}$ (Shigesada and Kawasaki 1997), where $\bar{\alpha} = \bar{\mu}\langle\frac{\alpha}{\mu}\rangle$ and $\alpha = \beta\tilde{S} - \lambda$. The number, N, of deer for a steady state population with density $\tilde{S} = \frac{K}{\mu}$, is given by

$$N = \iint_A \frac{K}{\mu}\, dA = K \iint_A \frac{1}{\mu}\, dA = KA\left\langle\frac{1}{\mu}\right\rangle, \tag{47}$$

where A is the area of the region of interest. Then $K = \frac{\bar{\mu}N}{A}$ and the wave speed becomes

$$v \approx 2\sqrt{\bar{\mu}^2\left\langle\frac{\frac{\beta\bar{\mu}N}{A\mu} - \lambda}{\mu}\right\rangle} = 2\bar{\mu}\sqrt{\left\langle\frac{\beta\bar{\mu}N}{A\mu^2} - \frac{\lambda}{\mu}\right\rangle}. \tag{48}$$

The value of N for which

$$\left\langle\frac{\beta\bar{\mu}N}{A\mu^2} - \frac{\lambda}{\mu}\right\rangle = \frac{\beta N\bar{\mu}}{A}\left\langle\frac{1}{\mu^2}\right\rangle - \lambda\left\langle\frac{1}{\mu}\right\rangle = 0 \tag{49}$$

is

$$N = \frac{\lambda A}{\beta}\left\langle\frac{1}{\mu}\right\rangle^2\left\langle\frac{1}{\mu^2}\right\rangle^{-1}. \tag{50}$$

For our study area, using the values for β, λ, and μ given in Sect. 4, the critical population would be $N = 12{,}447$. The current population is estimated at 7400 deer with a goal of 13,000 (U.D.W.R. 2010). If the infection rate, $\beta = 0.0326$, is appropriate for CWD in the La Sal mountains, the current deer population is less than the critical population suggesting that the disease will not spread out of the area. If the number of deer approaches the goal of 13,000 animals, however, the critical population would be exceeded and the wave speed would no longer be zero. It is important to note that this critical population was determined with an infection rate calculated from data for disease spread in a captive herd, scaled down a factor of 10 for the larger ranges of wild deer (Miller et al. 2006). If, for example, the infection rate is 10 times larger ($\beta = 0.326$, as fitted by Miller et al.), the critical population would be 1,245 deer, far below the present population, indicating that the disease can spread through the study area. We will revisit this idea with the more disease-specific model.

The homogenization procedure we have described will be invaluable in simulations of more complex models over large areas. In fact, the homogenization of ecological diffusion can be applied to many spatial invasion and dispersal models as well as spatial epidemiology models, when the effect of heterogeneous landscapes

on spread is desired. Homogenization preserves small scale variability while allowing computation on a large scale.

Acknowledgements Funding for this study was provided through USGS 1434-06HQRU1555. The authors would like to thank Mary Connor and John Lowry for providing data and advice.

Appendix: Numerical Method

For the non-homogenized model (4), let the spatial step be the same in both directions, i.e., $h = \Delta y_1 = \Delta y_2$, and let $k = \Delta\tau$. An alternating direction implicit (ADI) method for the non-homogenized model (4) has two equations for each time step, a discretization in the y_1-direction and a discretization in the y_2-direction:

$$\begin{aligned}
&I_{l,m}^{n+\frac{1}{2}} - \frac{k}{2h^2}\left(\mu_{l+1,m} I_{l+1,m}^{n+\frac{1}{2}} - 2\mu_{l,m} I_{l,m}^{n+\frac{1}{2}} + \mu_{l-1,m} I_{l-1,m}^{n+\frac{1}{2}}\right) - \frac{k}{2}\alpha_{l,m} I_{l,m}^{n+\frac{1}{2}} \\
&\quad = I_{l,m}^{n} + \frac{k}{2h^2}\left(\mu_{l,m+1} I_{l,m+1}^{n} - 2\mu_{l,m} I_{l,m}^{n} + \mu_{l,m-1} I_{l,m-1}^{n}\right) + \frac{k}{2}\alpha_{l,m} I_{l,m}^{n}, \\
&I_{l,m}^{n+1} - \frac{k}{2h^2}\left(\mu_{l,m+1} I_{l,m+1}^{n+1} - 2\mu_{l,m} I_{l,m}^{n+1} + \mu_{l,m-1} I_{l,m-1}^{n+1}\right) - \frac{k}{2}\alpha_{l,m} I_{l,m}^{n+1} \\
&\quad = I_{l,m}^{n+\frac{1}{2}} + \frac{k}{2h^2}\left(\mu_{l+1,m} I_{l+1,m}^{n+\frac{1}{2}} - 2\mu_{l,m} I_{l,m}^{n+\frac{1}{2}} + \mu_{l-1,m} I_{l-1,m}^{n+\frac{1}{2}}\right) + \frac{k}{2}\alpha_{l,m} I_{l,m}^{n+\frac{1}{2}}.
\end{aligned}$$

The superscript is the index for time, the first subscript is the index for y_1 and the second subscript is the index for y_2. Note that the motility coefficient, μ, is included inside of the central difference formula, since it is inside the Laplacian in (4).

For the homogenized model (23), let $h = \Delta x_1 = \Delta x_2$ and let $k = \Delta t$. Then the ADI method equations become

$$\begin{aligned}
&c_{l,m}^{n+\frac{1}{2}} - \frac{k}{2h^2}\bar{\mu}_{l,m}\left(c_{l+1,m}^{n+\frac{1}{2}} - 2c_{l,m}^{n+\frac{1}{2}} + c_{l-1,m}^{n+\frac{1}{2}}\right) - \frac{k}{2}\bar{\alpha}_{l,m} c_{l,m}^{n+\frac{1}{2}} \\
&\quad = c_{l,m}^{n} + \frac{k}{2h^2}\bar{\mu}_{l,m}\left(c_{l,m+1}^{n} - 2c_{l,m}^{n} + c_{l,m-1}^{n}\right) + \frac{k}{2}\bar{\alpha}_{l,m} c_{l,m}^{n}, \\
&c_{l,m}^{n+1} - \frac{k}{2h^2}\bar{\mu}_{l,m}\left(c_{l,m+1}^{n+1} - 2c_{l,m}^{n+1} + c_{l,m-1}^{n+1}\right) - \frac{k}{2}\bar{\alpha}_{l,m} c_{l,m}^{n+1} \\
&\quad = c_{l,m}^{n+\frac{1}{2}} + \frac{k}{2h^2}\bar{\mu}_{l,m}\left(c_{l+1,m}^{n+\frac{1}{2}} - 2c_{l,m}^{n+\frac{1}{2}} + c_{l-1,m}^{n+\frac{1}{2}}\right) + \frac{k}{2}\bar{\alpha}_{l,m} c_{l,m}^{n+\frac{1}{2}},
\end{aligned}$$

where the coefficients, $\bar{\mu}$ and $\bar{\alpha} = \bar{\mu}\langle\frac{\alpha}{\mu}\rangle$ are the averaged coefficients in (23). The homogenization procedure brings the motility coefficient outside of the Laplacian, so $\bar{\mu}$ remains outside of the central difference formula.

References

Andro, D. A., Karieva, P. M., Levin, S. A., & Okubo, A. (1990). Spread of invading organisms. *Landsc. Ecol.*, *4*, 177–188.

Baeten, L. A., Powers, B. E., Jewell, J. E., Spraker, T. R., & Miller, M. W. (2007). A natural case of chronic wasting disease in a free-ranging moose (*Alces alces shirasi*). *J. Wildl. Dis.*, *43*, 309–314.

Demaret, L., Eberl, H. J., Efendiev, M. A., & Maloszewski, P. (2009). A simple bioclogging model that accounts for spatial spread of bacteria. *Electron. J. Differ. Equ.*, *17*, 51–69.

Dewhirst, S., & Lutscher, F. (2009). Dispersal in heterogeneous habitats: thresholds, spatial scales, and approximate rates of spread. *Ecology*, *90*, 1338–1345.

Fisher, R. A. (1937). The wave of advance of advantageous genes. *Ann. Eugenics*, *7*, 355–369.

Fitzgibbon, W. E., Langlais, M., & Morgan, J. J. (2001). A mathematical model of the spread of feline leukemia virus (FeLV) through a highly heterogeneous spatial domain. *SIAM J. Math. Anal.*, *33*, 570–588.

Holmes, E. E., Lewis, M. A., Banks, J. E., & Veit, R. R. (1994). Partial differential equations in ecology: spatial interactions and population dynamics. *Ecology*, *75*, 17–29.

Holmes, M. H. (1995). *Introduction to perturbation methods*. New York: Springer.

Homer, C., Dewitz, J., Fry, J., Coan, M., Hossain, N., Larson, C., Herold, N., McKerrow, A., VanDriel, J. N., & Wickham, J. (2007) Completion of the 2001 National land cover database for the Conterminous United States. *Photogramm. Eng Remote Sens.*, *73*, 337–341.

Hooten, M. B., Garlick, M. J., & Powell, J. A. (2009). Advantageous change of support in inverse implementations of statistical differential equation models. In *JSM proceedings, section on Bayesian statistical science* (pp. 1847–1857). Alexandria: American Statistical Association.

Johnson, C. J., Pederson, J. A., Chappell, R. J., McKenzie, D., & Aiken, J. M. (2006). Oral transmissibility of prion disease is enhanced by binding to soil particles. *Pub. Library Sci. Pathogens*, *3*, 874–881.

Kallen, A., Arcui, P., & Murray, J. D. (1985). A simple model for spatial spread and control of rabies. *J. Theor. Biol.*, *116*, 377–393.

Kareiva, P., & Odell, G. (1987). Swarms of predators exhibit "preytaxis" if individual predators use area-restricted search. *Am. Nat.*, *130*, 233–270.

Kierstead, H., & Slobodkin, L. B. (1953). The size of water masses containing plankton bloom. *J. Mar. Res.*, *12*, 141–147.

Kinezaki, N., Kawasaki, K., Takasu, F., & Shigesada, N. (2003). Modeling biological invasions into periodically fragmented environments. *Theor. Popul. Biol.*, *64*, 291–302.

Lewis, M. A., Hillen, T., & Lutscher, F. (2005). Spatial dynamics in ecology. *IAS/Park City Math. Ser.*, *15*, 3–21.

Logan, D. J. (2006). *Applied mathematics* (3rd ed.). Hoboken: Wiley-Interscience.

McFarlane, L. R. (2007). *Breeding behavior and space use of male and female mule deer: An examination of potential risk differences for chronic wasting disease infection*. Master's thesis, Utah State University.

Meade, D. B., & Milner, F. A. (1992). *Applied mathematics monographs: Vol. 3. SIR epidemic models with directed diffusion*.

Miller, M. W., Williams, E. S., Hobbs, N. T., & Wolfe, L. L. (2004). Environmental sources of prion transmission in mule deer. *Emerg. Infect. Dis.*, *10*, 1003–1006.

Miller, M. W., Hobbs, N. T., & Tavener, S. J. (2006). Dynamics of prion disease transmission in mule deer. *Ecol. Appl.*, *16*, 2208–2214.

Miller, M. W., Swanson, H. M., Wolfe, L. L., Quartarone, F. G., Huwer, S. L., Southwick, C. H., & Lukacs, P. M. (2008). Lions, prions and deer demise. *Public Libr. Sci. ONE*, *3*, 1–7.

Mitchell, A. R., & Griffiths, D. F. (1980). *The finite difference method in partial differential equations*. Norwich: Wiley.

Murray, J. D. (1980). On pattern formation mechanisms for Lepidopteran wing patterns and mammalian coat markings. *Philos. Trans. R. Soc. Ser. B*, *295*, 473–496.

Okubo, A. (1980). *Diffusion and ecological problems: mathematical models*. New York: Springer.

Powell, J. A., & Zimmermann, N. E. (2004). Multiscale analysis of active seed dispersal contributes to resolving Reid's paradox. *Ecology*, *85*, 490–506.

Risken, H. (1986). *The Fokker–Planck equation: methods of solutions and applications*. Berlin: Springer.

Shigesada, N., & Kawasaki, K. (1997). *Biological invasions: theory and practice*. Oxford: Oxford University Press.

Shellam, J. G. (1951). Random dispersal in theoretical populations. *Biometrika*, *38*, 196–218.

Swindale, N. W. (1980). A model for the formation of ocular dominance stripes. *Proc. R. Soc. Lond. Ser. B*, *208*, 243–264.

Turchin, P. (1998). *Quantitative analysis of movement*. Sunderland: Sinauer.

Turing, A. M. (1952). The chemical basis of morphogenesis. *Philos. Trans. R. Soc. Lond. Ser. B*, *237*, 37–72.
U.D.W.R. (2010). Utah Division of Wildlife Resources Wildlife News: Ideal weather could mean a few more deer. http://wildlife.utah.gov.
Williams, E. S. (2005). Chronic wasting disease. *Vet. Pathol.*, *42*, 530–549.
With, K. A. (2002). The Landscape ecology of invasive spread. *Conserv. Biol.*, *16*, 1192–1203.